

Electronic Supporting Information

A highly sensitive and selective chemosensors for Cu²⁺ and Al³⁺ based on photoinduced electron transfer (PET) mechanism

Santosh Chemate, Nagaiyan Sekar*

Tinctorial Chemistry Group, Department of Dyestuff Technology, Institute of Chemical Technology (Formerly UDCT), N. P. Marg, Matunga, Mumbai - 400 019.

Email: n.sekar@ictmumbai.edu.in, nethi.sekar@gmail.com

Table of contents:

1. Supplementary spectral data

Fig. S1 and Fig. S2 -----	2
Fig. S3 and Fig. S4 -----	3
Fig. S5-----	4
Fig. S6-----	5
Fig. S7-----	6
Fig. S8-----	7
Fig. S9-----	8

2. The characterization data of compound 7a and 7b

¹ H NMR spectra of 7a -----	9
¹³ C NMR spectra of 7a -----	10
¹ H NMR spectra of 7b -----	11
¹³ C NMR spectra of 7b -----	12
¹ H NMR spectra of 7a-Cu ²⁺ (1:1) in DMSO- <i>d</i> 6-----	13
¹ H NMR spectra of 7b-Al ³⁺ (1:1) in DMSO- <i>d</i> 6-----	14

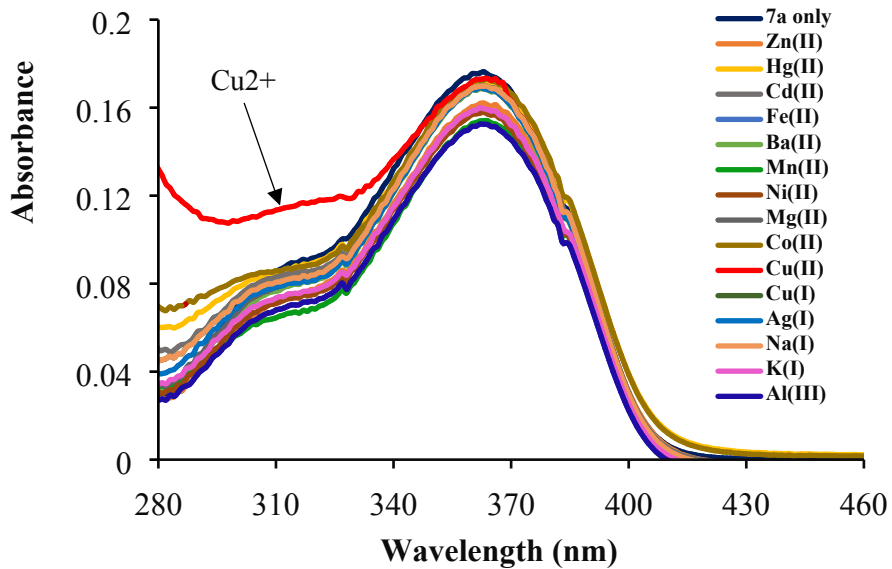


Fig. S1. Absorption spectra of **7a** (20 μM) upon addition of Zn^{2+} , Hg^{2+} , Cd^{2+} , Fe^{2+} , Ba^{2+} , Mn^{2+} , Ni^{2+} , Mg^{2+} , Co^{2+} , Cu^{2+} , Cu^+ , Ag^+ , Na^+ , K^+ and Al^{3+} (5 equiv.) in CH_3CN .

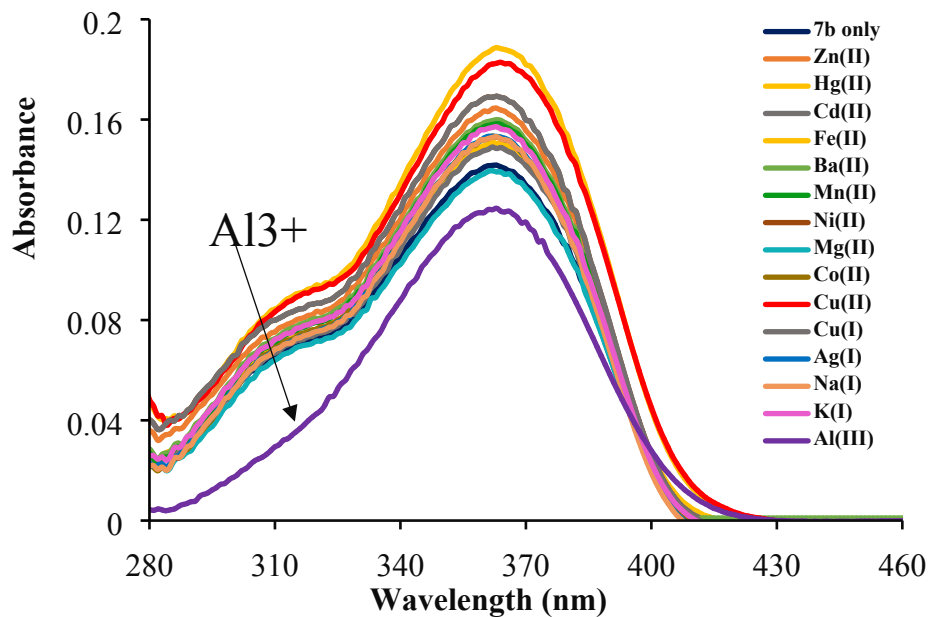


Fig. S2. Absorption spectra of **7b** (20 μM) upon addition of Zn^{2+} , Hg^{2+} , Cd^{2+} , Fe^{2+} , Ba^{2+} , Mn^{2+} , Ni^{2+} , Mg^{2+} , Co^{2+} , Cu^{2+} , Cu^+ , Ag^+ , Na^+ , K^+ and Al^{3+} (5 equiv.) in CH_3CN .

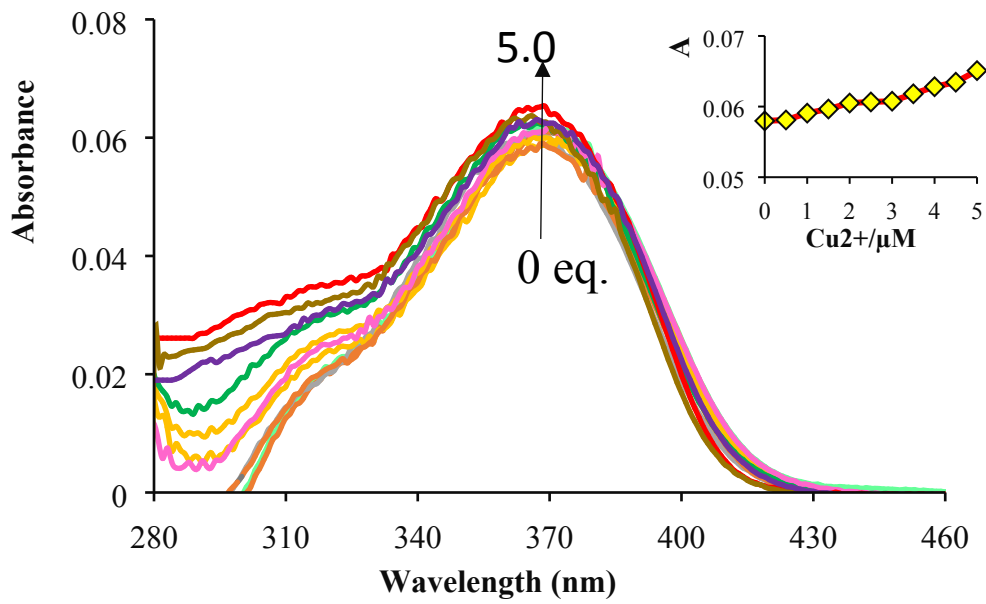


Fig. S3. Changes in the absorption spectra of probe **7a** (10 μM) upon titration with 0 to 5.0 eq. of Cu^{2+} in CH_3CN . Inset: Absorbance at 365 nm as a function of Cu^{2+} concentration.

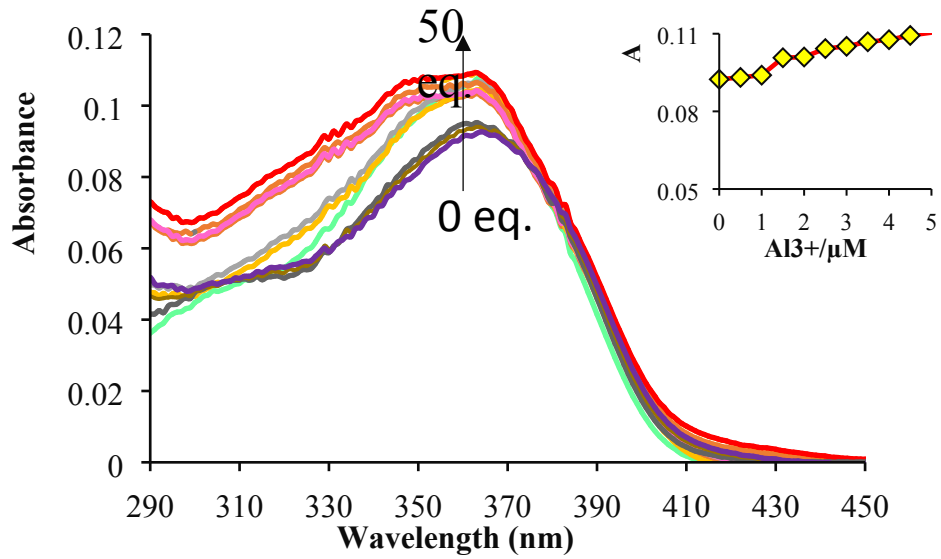


Fig. S4. Changes in the absorption spectra of probe **7b** (10 μM) upon titration with 0 to 5.0 eq. of Al^{3+} in CH_3CN . Inset: Absorbance at 365 nm as a function of Al^{3+} concentration.

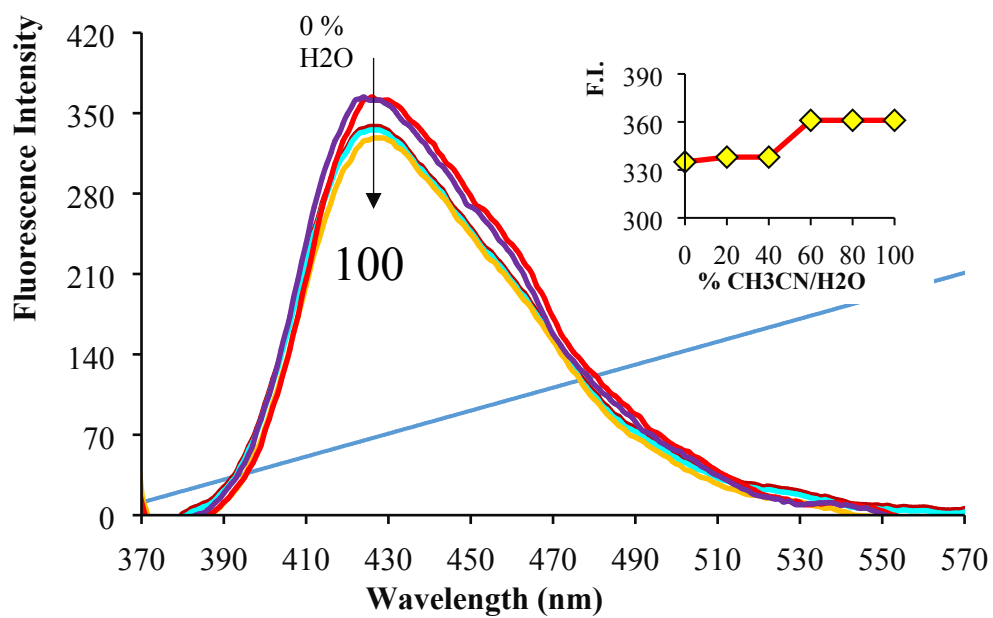


Fig. S5. Change in the fluorescence emission spectra of probe **7a** (10 μM) in $\text{CH}_3\text{CN}/\text{H}_2\text{O}$ mixture upon titration with 5.0 eq. of Cu^{2+} at pH 9.0. Inset: The fluorescence intensity (F.I.) at 428 nm as a function of $\text{CH}_3\text{CN}/\text{H}_2\text{O}$ mixture. $\lambda_{\text{ex}} = 365 \text{ nm}$ (Slit widths: 2.5 nm/2.5 nm).

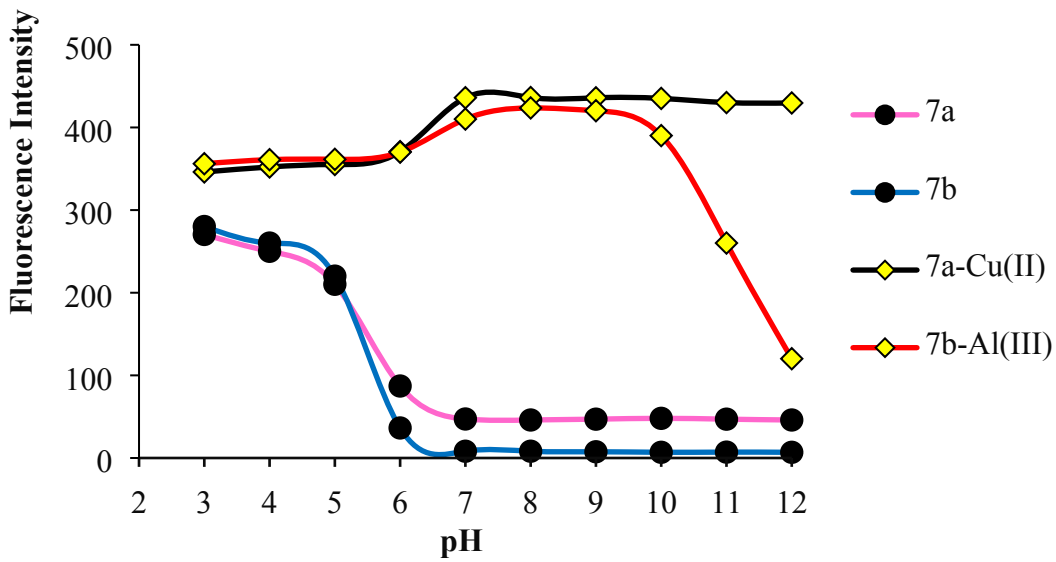


Fig. S6. Fluorescence response of free chemosensor **7a** (10.0 μM) and after addition of Cu^{2+} (10.0 μM) and **7b** (10.0 μM) and after addition of Al^{3+} (10.0 μM) in ACN-Phosphate buffer (10 mM, 9:1, v/v) as a function of different pH values. $\lambda_{\text{ex}} = 365 \text{ nm}$ (Slit widths: 5 nm/5 nm).

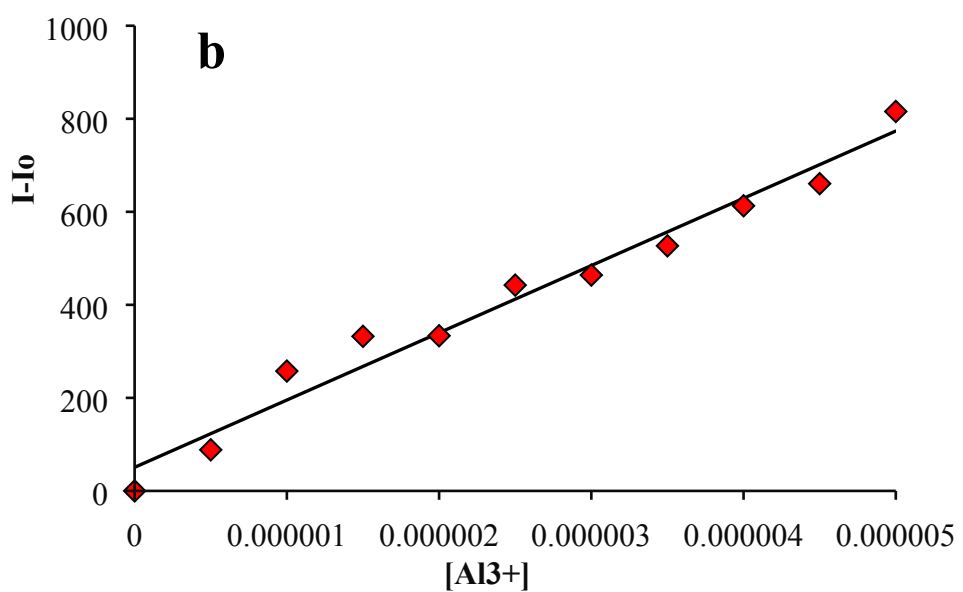
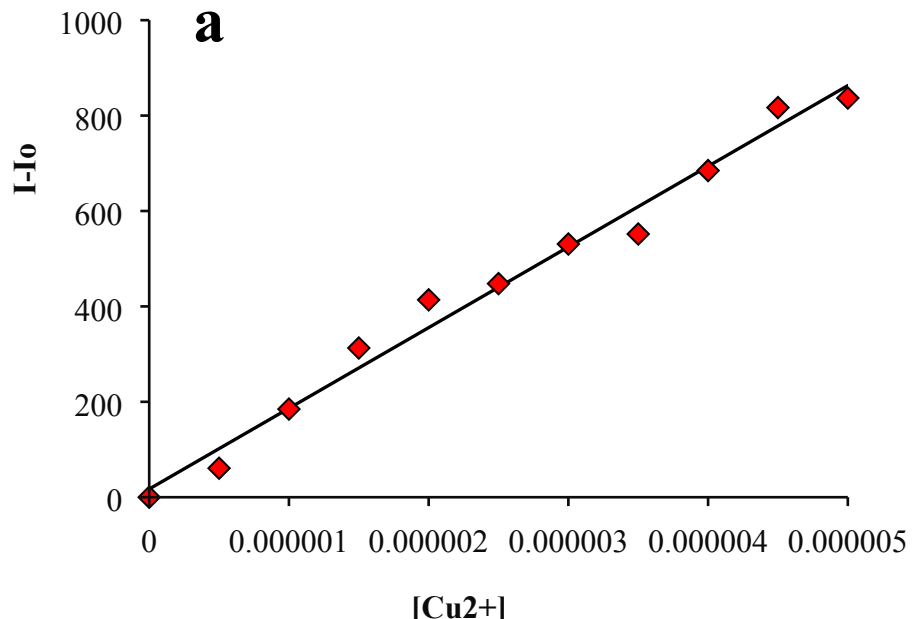


Fig. S7. Limit of detection calculation for **7a-Cu²⁺** (a) and **7b-Al³⁺** (b) complexes from linear curve fit of emission values.

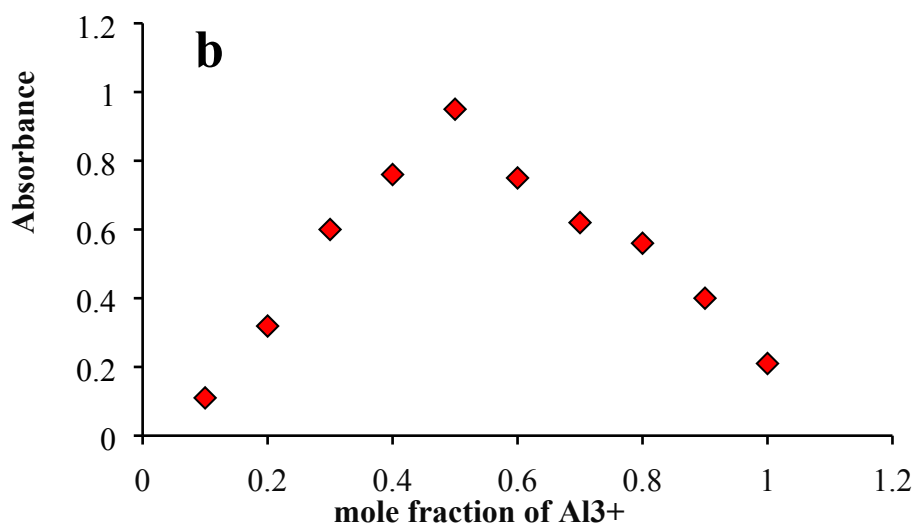
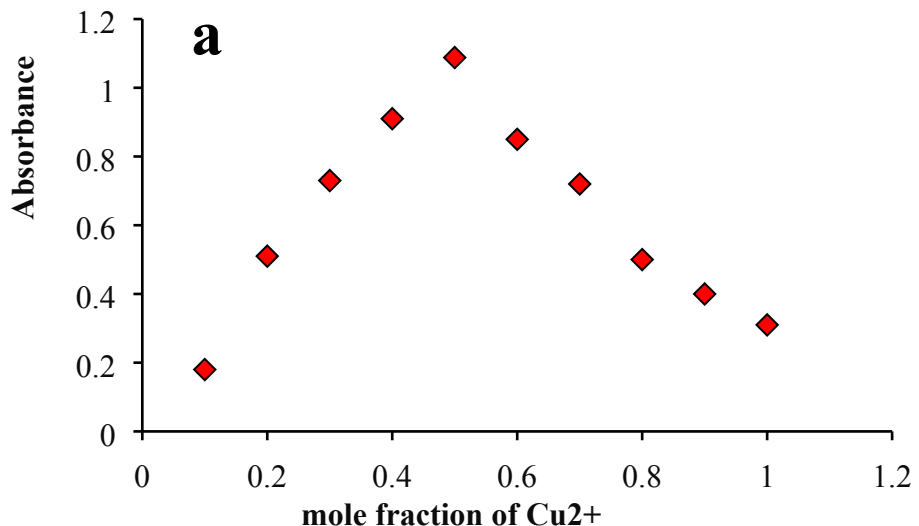


Fig. S8. Job's plot of the (a) **7a**- Cu^{2+} and (b) **7b**- Al^{3+} complexes in CH_3CN . The total concentration of L-metal was 1.0×10^{-4} M.

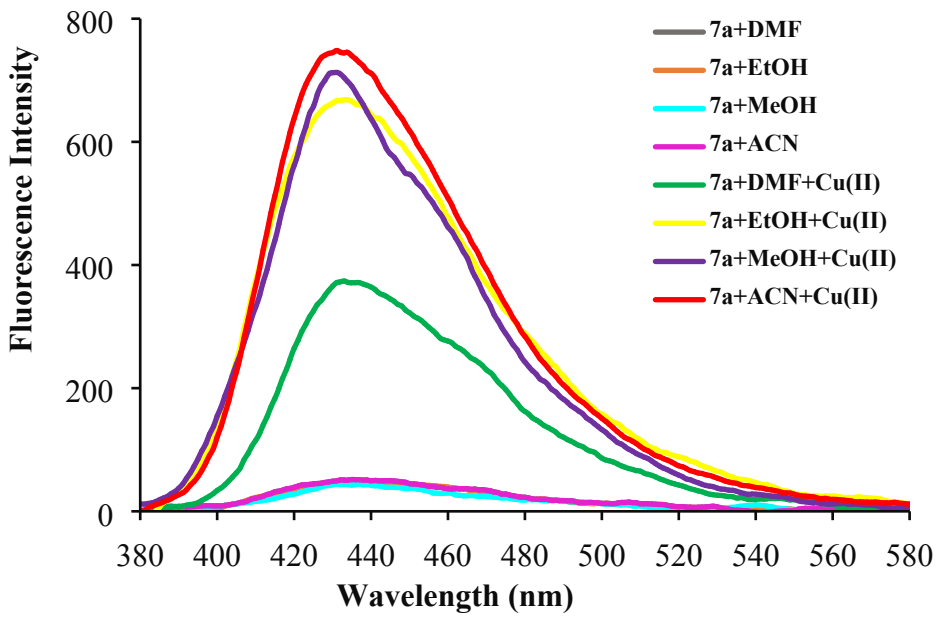


Fig. S9. Effect of the solvents on the fluorescence intensity of **7a** (20 μ M) in the presence or absence of Cu²⁺ ions (5 equiv.). $\lambda_{\text{ex}} = 365$ nm (Slit widths: 5 nm/5 nm).

7a

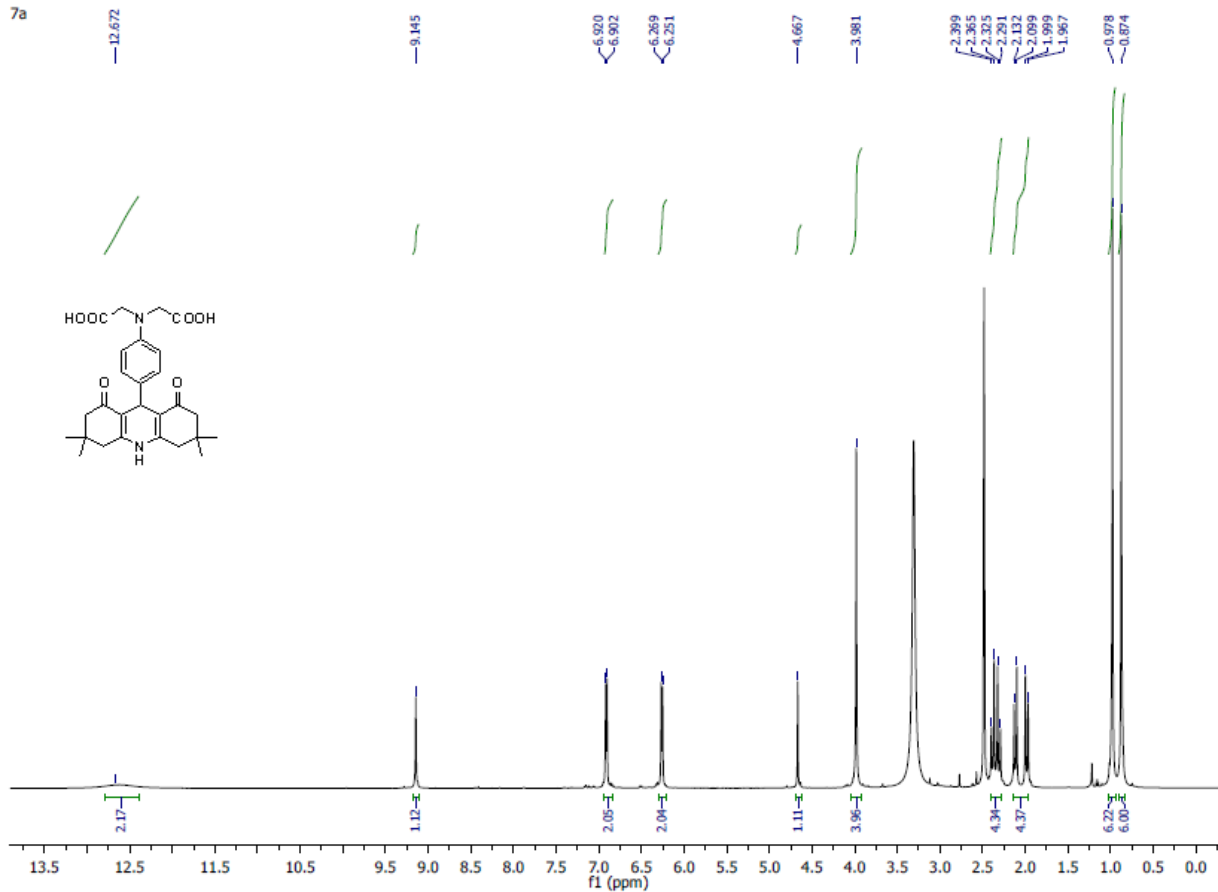


Fig. S10. ^1H NMR spectra of 7a in $\text{DMSO}-d_6$.

7a

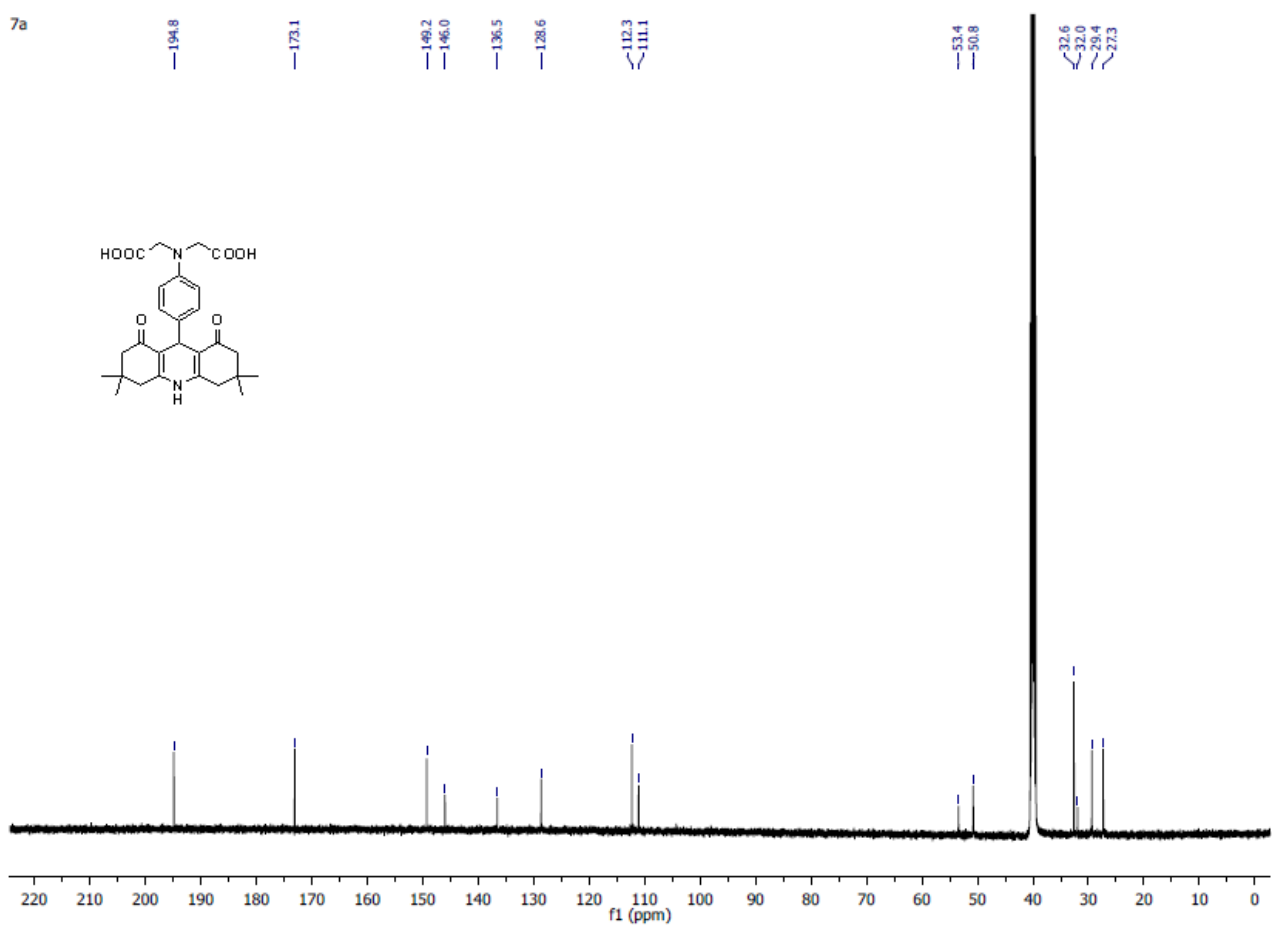


Fig. S11. ^{13}C NMR spectra of 7a in $\text{DMSO}-d_6$.

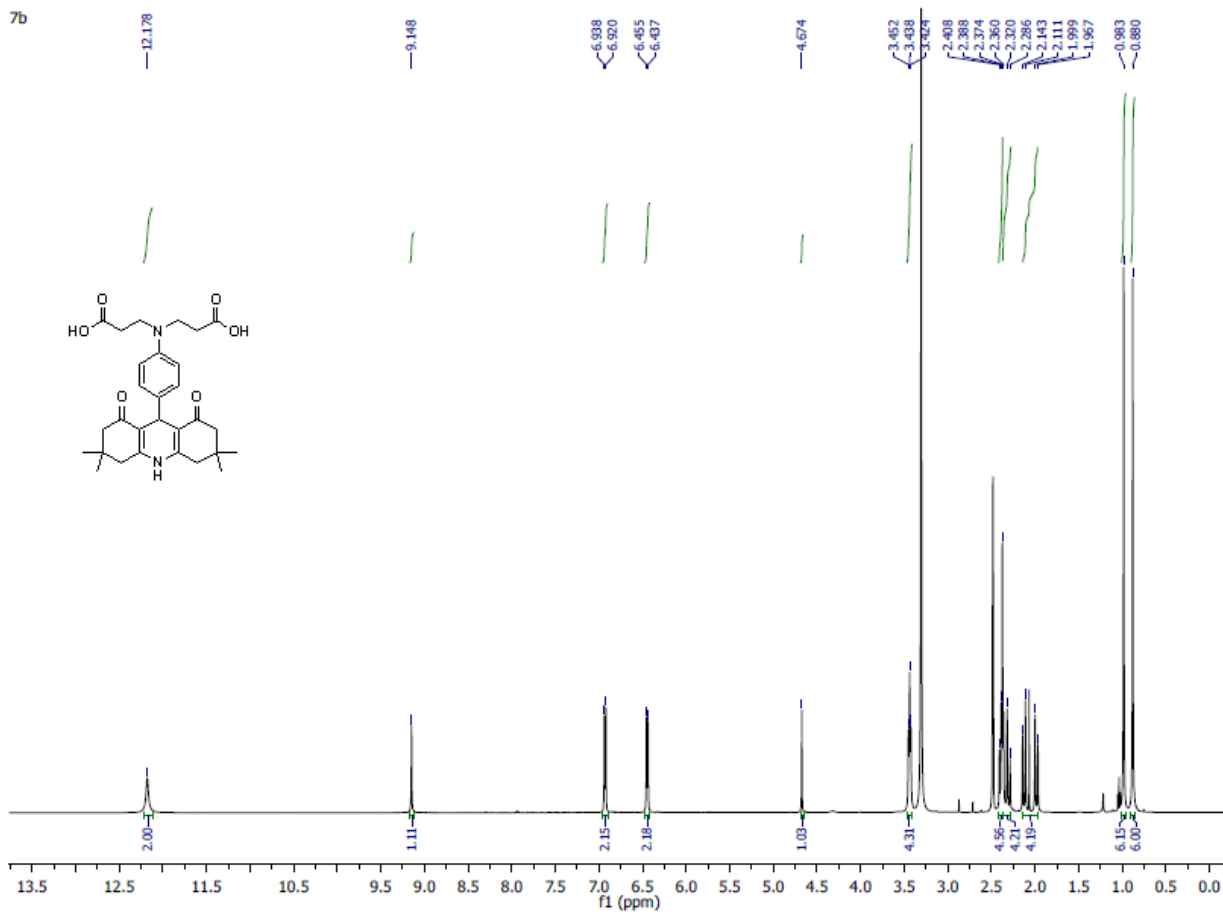


Fig. S12. ^1H NMR spectra of **7b** in $\text{DMSO}-d_6$.

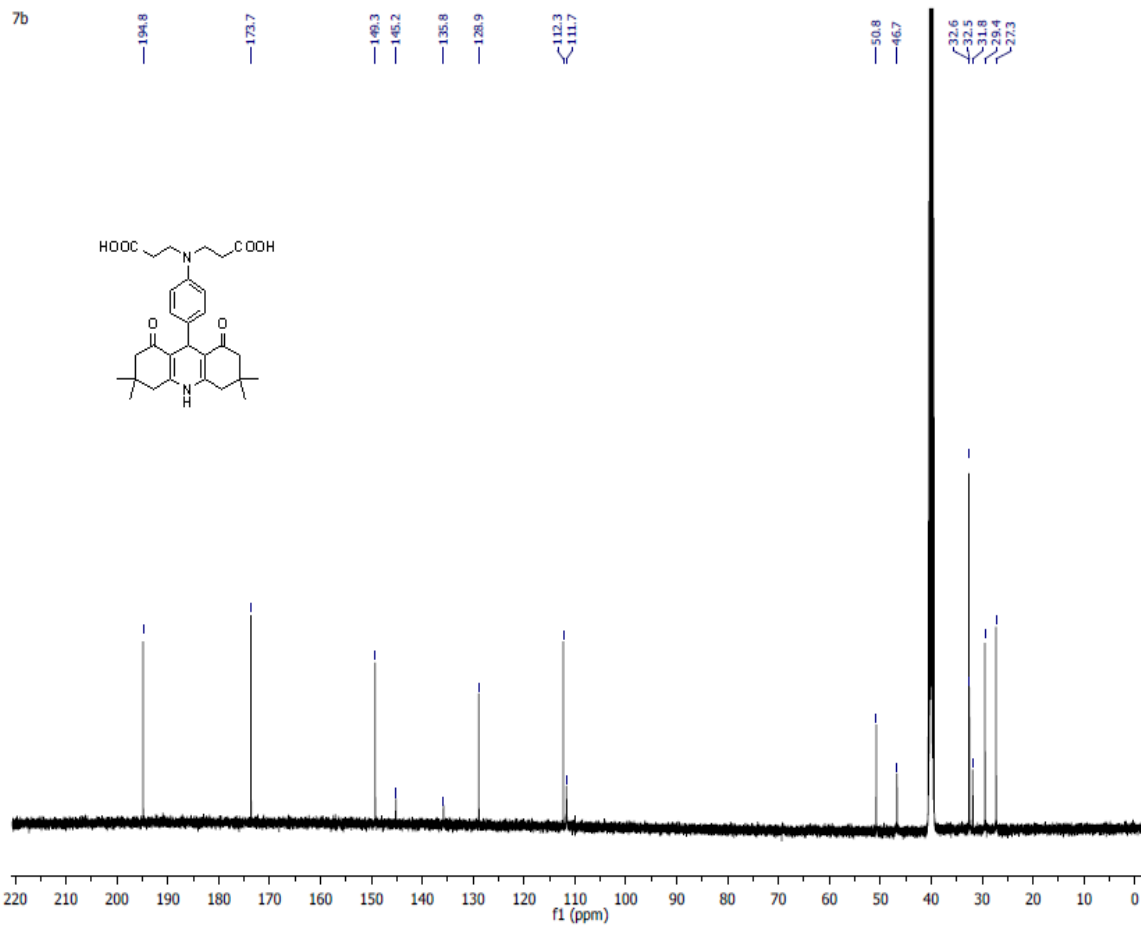


Fig. S13. ^{13}C NMR spectra of **7b** in $\text{DMSO}-d_6$.

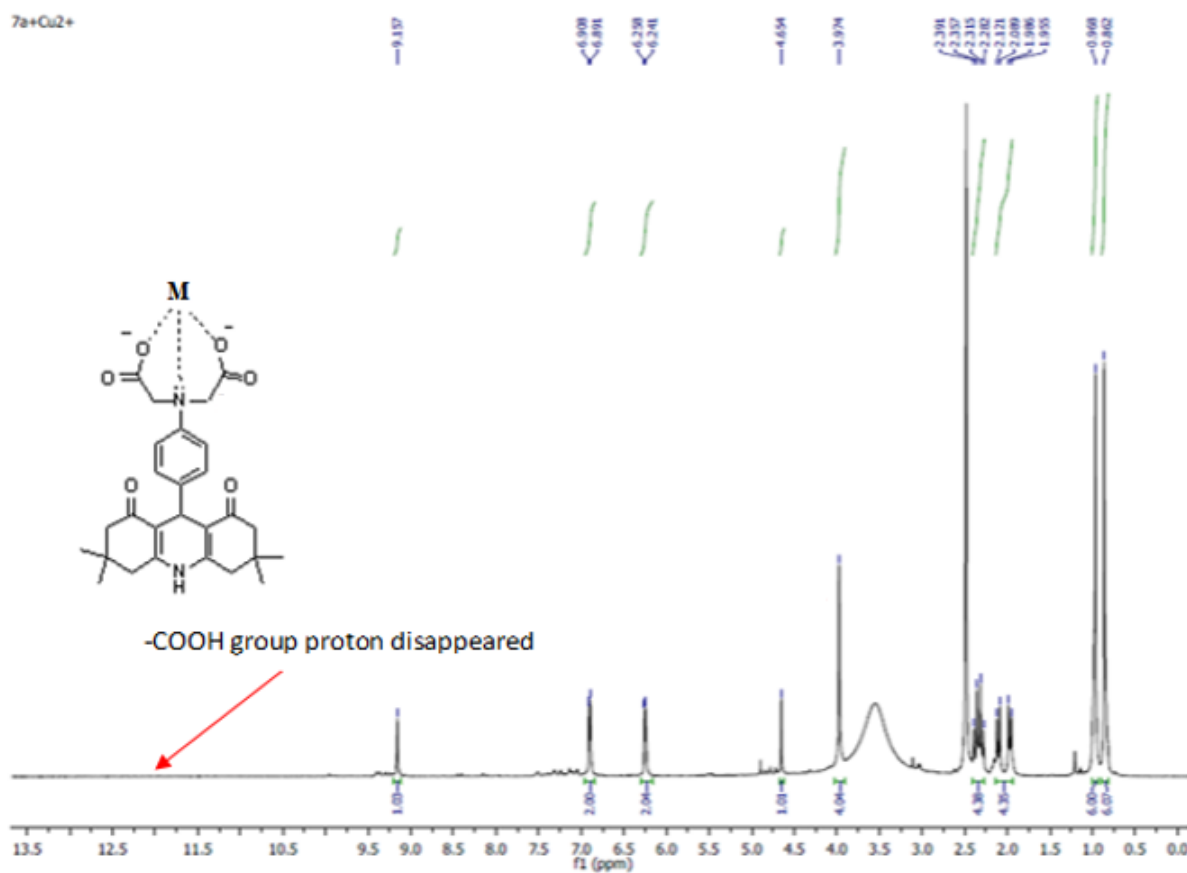


Fig. S14. ¹H NMR spectra of 7a-Cu²⁺ (1:1) in DMSO-d6.

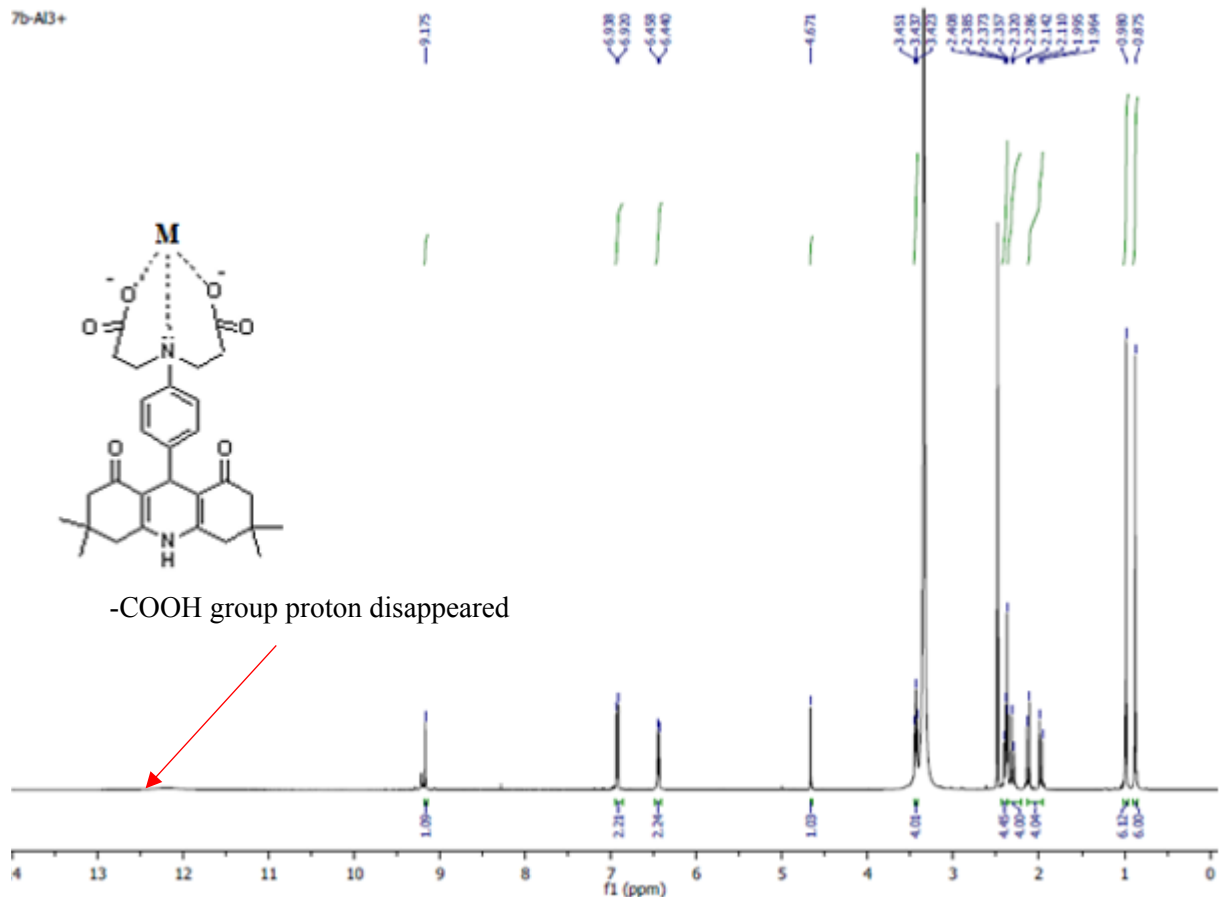


Fig. S15. ^1H NMR spectra of **7b-Al³⁺** (1:1) in DMSO-*d*6.